Spin dynamics and charge order in β−Na1/3V2O5

M. Heinrich, Hans-Albrecht Krug von Nidda, R. M. Eremina, Alois Loidl, Christian Helbig, Günter Obermeier, Siegfried R. Horn

Angaben zur Veröffentlichung / Publication details:

Heinrich, M., Hans-Albrecht Krug von Nidda, R. M. Eremina, Alois Loidl, Christian Helbig, Günter Obermeier, and Siegfried R. Horn. 2004. "Spin dynamics and charge order in β−Na1/3V2O5." *Physical Review Letters* 93 (11): 116402. https://doi.org/10.1103/physrevlett.93.116402.

Spin Dynamics and Charge Order in $\beta - Na_{1/3}V_2O_5$

M. Heinrich,[1] H.–A. Krug von Nidda,[1] R. M. Eremina,[2,1] A. Loidl,[1] Ch. Helbig,[1] G. Obermeier,[1] and S. Horn[1]

[1]*Institute of Physics, University of Augsburg, 86135 Augsburg, Germany*
[2]*E. K. Zavoisky Physical-Technical Institute, 420029 Kazan, Russia*

(Received 15 April 2004; published 10 September 2004)

We present detailed electron-spin resonance investigations on single crystals of the one-dimensional vanadium-oxide bronze $\beta - Na_{1/3}V_2O_5$. From the angular dependence of the g value it can be concluded that the electrons are primarily located on the V1 zigzag chains. The anisotropy of the linewidth, which is determined by the intrachain symmetric anisotropic exchange interaction, favors statistic electron distribution in the metallic and blockwise charge-order in the insulating phase. The temperature dependence of the linewidth indicates the opening of a charge gap at the metal-to-insulator transition at $T_{MI} = 132$ K.

DOI: 10.1103/PhysRevLett.93.116402 PACS numbers: 71.30.+h, 72.80.Ga, 73.90.+f, 76.30.–v

The recent discovery of a metal-to-insulator transition (MIT) [1] and of superconductivity under high pressure [2] in $\beta - Na_{1/3}V_2O_5$ renewed the interest in this one-dimensional (1D) compound. A series of investigations started to clarify the origin of the MIT, which can be only observed in stoichiometric samples. Already small deviations of the Na concentration $x = 1/3$ inhibit the existence of the metallic phase and lead to semiconducting behavior [1]. The monoclinic crystal structure ($C2/m$, space group 12) of $\beta - Na_{1/3}V_2O_5$ is highly anisotropic. Three inequivalent vanadium sites (V1, V2, V3) build three kinds of chains along the crystallographic b direction [3,4] as illustrated in Fig. 1: The V1 sites form zigzag chains of edge-sharing VO_6 octahedra, the V2 sites build two-leg ladders of corner-sharing VO_6 octahedra, and the V3 sites lie on zigzag chains of edge-sharing VO_5 square pyramids. Within this V_2O_5 framework the Na sites are located in tunnels along the b direction. Each Na atom donates one electron to the empty vanadium d bands and consequently the ratio of V^{4+} ($3d^1$: $S = 1/2$) to V^{5+} ($3d^0$: $S = 0$) is 1:5. In $\beta - Na_{1/3}V_2O_5$ only one of the two closely spaced Na sites of the unit cell is occupied revealing a zigzag chain within each tunnel. These chains develop a long-range order below 230 K leading to a doubling of the unit cell along the b axis [5]. Two further phase transitions occur at lower temperatures: Antiferromagnetic long-range order at $T_N = 24$ K[1,6] and the MIT at $T_{MI} = 132$ K [1] accompanied by an additional tripling of the b axis [7]. The ordered state at low temperatures is a canted antiferromagnet with the spontaneous magnetization along the b axis [8,9].

The nature of the MIT in $\beta - Na_{1/3}V_2O_5$ has not been clarified yet. Both the conduction mechanism and the charge distribution are heavily under debate. According to NMR measurements the electrons can occupy all three vanadium sites above T_{MI} [6,9] revealing a rather ionic state of V3 with respect to mixed valent V1 and V2 sites responsible for the metallic behavior. Recent optical investigations revealed a strong electron-phonon coupling, which supports the picture that the charge carriers in $\beta - Na_{1/3}V_2O_5$ should be regarded as small polarons [10]. Photoemission spectroscopy suggests that the electrons occupy either the V2 ladder, the V1 zigzag chain, or both simultaneously [11]. Below T_{MI} the insulating state is a charge-ordered phase and different charge-order (CO) scenarios were proposed: NMR Knight shift and magnetic properties indicate the condensation of the electrons on V1 or V2 sites [6,9]. Theoretical calculations predicted a linear chain of electrons on V1 sites [12], while in contrast x-ray diffraction provided evidence of a block-

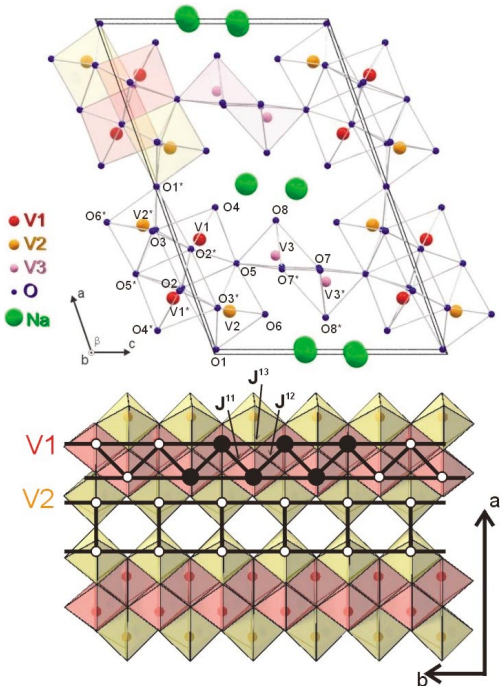

FIG. 1 (color online). Crystal structure of $\beta - Na_{1/3}V_2O_5$ and plot of V1 zigzag chain and V2 ladder. Black spheres denote electronically occupied V sites ($3d^1$) as derived from our ESR results. Stars indicate positions at $b/2$ above the ac plane.

wise occupation of V2 sites due to changes of the V2-O distances resulting in a $6b$ periodicity [7]. These contradictory conclusions call for further experiments on $\beta - Na_{1/3}V_2O_5$ to answer the open questions about the origin of the MIT and the CO pattern.

Electron-spin resonance (ESR) is ideally suited for the investigation of the magnetic properties of vanadium systems, since the V^{4+} ions with electron configuration $3d^1$ can be used as a microscopic probe of the spin system. A number of ESR investigations in $\beta - Na_{1/3}V_2O_5$ have been performed already about 20 years ago [13–16], but they did not reveal the signature of the MIT probably due to slight deviations from the ideal stoichiometry [1]. In contrast, we found a pronounced anomaly in the temperature dependence of the resonance linewidth near 132 K, which encouraged us to perform a detailed reinvestigation of the ESR in $\beta - Na_{1/3}V_2O_5$ single crystals of high quality. Sample preparation as well as susceptibility and resistivity measurements are presented in Ref. [5].

The ESR measurements were performed at a Bruker ELEXSYS E500-CW spectrometer equipped with continuous-flow He cryostats (Oxford Instruments) at X band (9.4 GHz) and Q band (34 GHz) frequencies in the temperature range 4.2-300 K. A needlelike $\beta - Na_{1/3}V_2O_5$ single crystal was oriented by means of single-crystal x-ray diffraction and then was fixed in a quartz tube with paraffin in selected orientations.

For all temperatures $T \geq T_N$ and orientations of the sample in the external magnetic field H the ESR spectra of $\beta - Na_{1/3}V_2O_5$ consist of a single resonance line of Lorentzian shape. Resonance field H_{res} and linewidth ΔH (half width at half maximum) have been determined by numerical fits to the spectra, as described, e.g., in Ref. [17]. Because of the antiferromagnetic ordering the signal shifts out of the available frequency range for temperatures below 24 K. A detailed description of the antiferromagnetic resonance can be found in Ref. [8].

The temperature-dependent behavior of ΔH and g was examined with the external magnetic field applied along the three crystallographic axes and along a^*, which is the direction perpendicular to the bc plane. The investigations at X-band and Q-band frequencies revealed identical results. Figure 2 presents the experimental data. There are three different temperature regimes: (i) Below 30 K the resonance line broadens and shifts to lower fields on approaching the magnetic transition at 24 K and vanishes for $T < T_N$. (ii) Between 30 K and 132 K the linewidth increases monotonously with increasing temperature. It reveals an inflection point near 100 K, and an exponential increase towards T_{MI} for all orientations of the sample simultaneously with the conductivity, which is also plotted in Fig. 2. The g values are constant in this temperature range for $H \parallel b$ and $H \parallel a$. For $H \parallel c$ it decreases slowly, for $H \parallel a^*$ it increases slightly. (iii) At the MIT at 132 K the linewidth exhibits a distinct kink for all orientations and approaches constant values on further increasing the

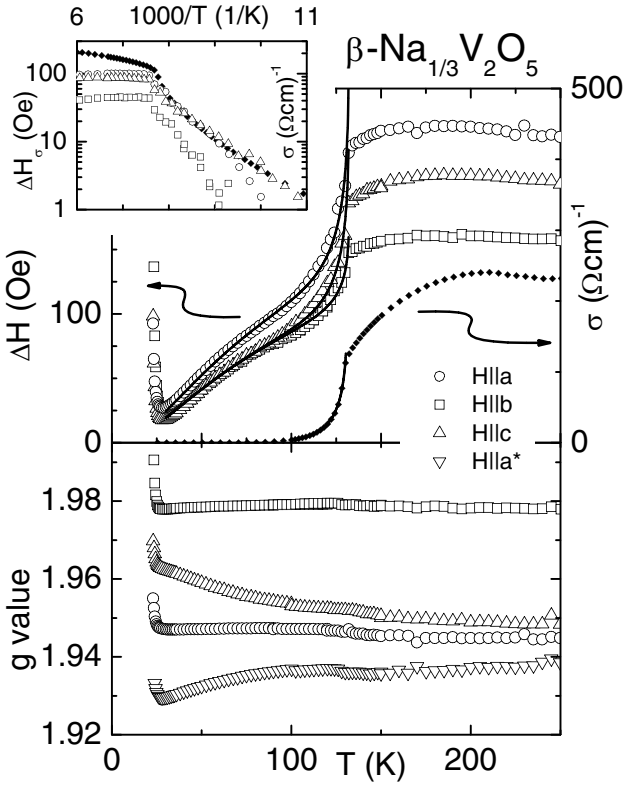

FIG. 2. Temperature dependence of ESR linewidth ΔH (Inset: reduced contribution ΔH_σ compared to b-axis conductivity as Arrhenius plot) and g value of a $\beta - Na_{1/3}V_2O_5$ single-crystal at Q-band frequency with the external magnetic field parallel to different crystallographic axes.

temperature. The g values are nearly unaffected by the phase transition and remain almost constant in the high temperature regime.

To characterize the metallic and the insulating phase we performed a detailed investigation of the orientation dependence far below and far above the MIT. Figure 3 shows the angular dependence of the linewidth and the g factor for three perpendicular crystallographic planes, namely, the a^*b, ac, and bc planes, at 50 and 200 K. Already at first sight it is evident that the anisotropy is modified only weakly by the phase transition. This indicates a strong relation between the electron occupation of the insulating and the metallic phase.

To simulate the angular variation of the g value the following local coordinate system was found to be appropriate: The local z axis is approximately parallel to the V1-O4 direction or V2-O6 direction, respectively, (see Fig. 1), the local y axis is aligned parallel to the crystallographic b axis, and the local x axis perpendicular to y and z. The experimental data at both temperatures were approximated by varying the molecular g values (see Table I and solid lines in Fig. 3). The obtained values slightly below the free electronic value $g = 2$ are typical for V^{4+} in distorted octahedral coordination [18]. The strongest shift is expected for the magnetic field applied parallel to the directions of the dominant uniaxial distortion.

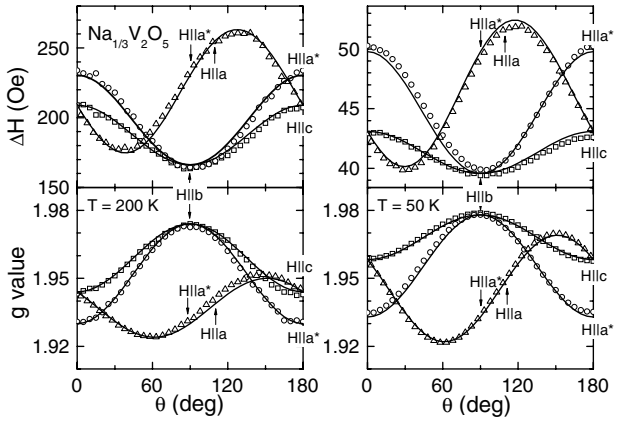

FIG. 3. Angular dependence of ESR linewidth ΔH and g value of a $\beta - Na_{1/3}V_2O_5$ single-crystal at 200 K and 50 K (X band). Solid lines: simulations (see text).

Definite conclusions about the electron distribution in $\beta - Na_{1/3}V_2O_5$ can be drawn considering the crystal structure: The shortest V1-O distance in the V1 octahedron is V1-O4, the shortest V2-O distance in the V2 octahedron is V2-O6. These directions indicate the main axis of distortion for the two sites. The strongest g shift is expected for the site, which primarily is occupied. The angle between these two directions is about 90°. Hence, if half of the electrons occupy the V1 sites and half of the electrons the V2 sites, rotation in the ac plane reveals a constant g value. However, since one observes a pronounced anisotropy in the ac plane and g_{zz} is the smallest molecular g value, the electrons occupy primarily the V1 sites. Consequently, according to these results more than 50% of the electrons are located on V1 sites above as well as below the MIT. The distinct anisotropy in the ac plane at low temperatures indicates that nearly all electrons occupy the V1 sites in agreement with [15]. With increasing temperature the observed anisotropy is strongly reduced as is also clearly visible in the temperature dependence of the g values plotted in Fig. 2. This suggests that in the metallic phase the electrons are more delocalized and can also occupy the V2 sites to a minor degree.

Further evidence on the distribution of charge can be derived from the anisotropy of the linewidth. The saturation of ΔH above T_{MI} indicates the dominance of spin-spin relaxation in the metallic phase. In case of strong exchange narrowing $\Delta H = \hbar M_2/(g\mu_B\omega_{ex})$ is determined by the angular-dependent second moments M_2, caused by the anisotropic spin-spin interactions, and the exchange frequency $\omega_{ex} \approx J/\hbar$ [19]. An estimation of the linewidth due to dipole-dipole, hyperfine, and anisotropic exchange (AE) interaction following [20] yields smaller values than experimentally observed. However, like in $LiCuVO_4$ [17] the ring-shaped exchange geometry might enhance the AE accordingly ($J_{AE} \approx 0.01J$). The similar anisotropy above and below the MIT implies that the same interaction is responsible for the line broadening in the insulating phase. For calculating the particular second moments $M_2(J^{ij})$ of the AE interactions J^{ij} dependent on the orientation of the external magnetic field we used the procedure specified in Refs. [17,21]. For both temperatures the data can be described considering exclusively the three possible exchange pathways within the V1 zigzag chain illustrated in Fig. 1. The principal axes of the corresponding AE tensors were chosen considering the bond geometry according to Ref. [22]: One principal axis (x) is aligned along the straight connection of nearest-neighboring V1 sites. The second axis (y) has to be chosen perpendicular to the plane spanned by the V ions and the connecting O ligands. The third axis (z) is perpendicular to both of them. The interchain interaction was neglected. The contributions of the single exchange interactions to the total second moment have to be weighted depending on the respective phase:

Since the electrons in the metallic phase are randomly distributed in the V1 zigzag chain the second moments resulting of the three particular contributions have to be averaged statistically as

$$M_2^{met} = \frac{M_2(J_{\alpha\beta}^{11}) + M_2(J_{\alpha\beta}^{12}) + 2M_2(J_{\alpha\beta}^{13})}{4}. \quad (1)$$

The solid lines in the upper left panel of Fig. 3 were obtained using the relative diagonal exchange-tensor components listed in Table I. The minor amount of electrons on the V2 sites was neglected.

Considering the available number of electrons and the variation of the V2-O1-V2 distance with every six rungs of the V2 ladder below the MIT [7] we assumed the following scenario for the insulating phase: As suggested in Fig. 1 by black spheres six consecutive sites of the V1 zigzag chain are occupied by electrons. So we have 5 times the interactions J^{11} and J^{12} and 8 times the interaction J^{13} due to the average of the two possible existing configurations:

$$M_2^{ins} = \frac{5M_2(J_{\alpha\beta}^{11}) + 5M_2(J_{\alpha\beta}^{12}) + 8M_2(J_{\alpha\beta}^{13})}{12} \quad (2)$$

The results are given in Table I and Fig. 3. Note that it is not possible to describe the anisotropy considering solely the linear interaction J^{13}, i. e., the anisotropy of the ESR linewidth contradicts a linear formation of electrons on the V1 sites. However, our six pack scenario is only a suggestion, because there might exist further electron

TABLE I. Relative diagonal anisotropic exchange-tensor components using the normalization $J_{xx}^{1i} + J_{yy}^{1i} + J_{zz}^{1i} = 0$ determined from fits on the angular dependence of ΔH. J^{11} and J^{12} are equivalent with other local coordinate systems.

	$\frac{J_{xx}^{11}}{J_{zz}^{11}}$	$\frac{J_{yy}^{11}}{J_{zz}^{11}}$	$\frac{J_{xx}^{13}}{J_{zz}^{13}}$	$\frac{J_{yy}^{13}}{J_{zz}^{13}}$	g_{xx}	g_{yy}	g_{zz}
50 K	−0.59	−0.41	0.57	−1.57	1.969	1.978	1.922
200K	−2/3	−1/3	0.75	−1.75	1.950	1.974	1.924

configurations compatible with the experimental results. In particular the formation of a charge-density wave with a sixfold periodicity may be a reasonable pattern.

In canonical spin chains with the line broadening dominated by the symmetric AE the linewidth increases monotonously at low temperatures approaching a saturation at high temperatures [23]. In the case of $\beta - Na_{1/3}V_2O_5$ the one dimensionality might be questioned due to the lack of the characteristic maximum in the susceptibility expected for a spin chain with $J/k_B = 120$ K. Nevertheless, the overall behavior resembles such a temperature law. Remarkably, the temperature dependence deviates from this canonical behavior near the MIT, where the AE is altered due to the delocalization of the electrons already below the phase transition indicated by the simultaneous increase of the conductivity σ. Between $100 < T < 132$ K the latter can be described by an exponential expression $\sim \exp[-\Delta(T)/k_B T]$ containing a temperature-dependent gap $\Delta(T) = 1.74\Delta_0(1 - \frac{T}{T_{MI}})^{0.5}$. This yields $\Delta_0 = 475$ K and the respective line in Fig. 2. Note that the gap value of 600 K in Ref. [5] has been determined for $T < 90$ K, whereas here we evaluated the same data set with respect to the behavior near T_{MI}.

To approximate the temperature-dependent linewidth below the MIT a second term has to be added due to the increase at lower temperatures. In other 1D antiferromagnets as, e. g., $CuGeO_3$, it has been possible to describe the canonical behavior empirically by an exponential function $\Delta H \sim \exp[-2C_1/k_B(T + C_2)]$, where $C_1 \approx J$ and C_2 is of the order of the ground-state transition temperature [21]. Since this expression gives the appropriate behavior, the data below 90 K were at first fitted exclusively with this chain contribution yielding $C_1 = 50 \pm 5$ K and $C_2 = 12 \pm 5$ K within the given error for different orientations. C_1 is only about half of the expected value but this should not be over interpreted regarding the complex CO phase. Then, subtracting the extrapolated fit curve from the data using the average values and plotting the result ΔH_σ together with the conductivity in Arrhenius representation reveals a convincing coincidence of both quantities near the MIT (see inset of Fig. 2). The fit of the sum of both contributions with the gap value obtained from σ is shown as solid lines in the main frame of Fig. 2. Thus, the ESR linewidth successfully probes the opening of the charge gap at the MIT. The ratio $2\Delta_0/k_B T_{MI} \approx 7.2$ is enhanced with respect to the mean-field value of 3.52 due to the dominance of fluctuations in one dimension [24]. This result immediately implies the possibility of a charge-density wave formation. However, the susceptibility does not show the concomitant formation of a spin gap at T_{MI}. This suggests the presence of a strong Coulomb onsite interaction, which may result in spin-charge separation for a partially occupied 1D chain.

In conclusion, using ESR techniques we have investigated the angular and temperature dependence of linewidth and g value on $\beta - Na_{1/3}V_2O_5$ single crystals. Important information can be derived: (i) The anisotropy of the g value yields a preferential occupation of the V1 sites both above and below T_{MI}. (ii) The temperature dependence of the g value allows for a minor occupation of the V2 sites, which reduces strongly below T_{MI}. (iii) From the anisotropy of the linewidth a linear CO pattern can be definitely excluded. Taking into account the sixfold lattice periodicity along b we suggest that in the insulating state the charges occupy six consecutive V1 sites within the V1 zigzag chain. (iv) The temperature dependence of the linewidth clearly indicates the opening of a charge gap in excellent agreement with conductivity measurements.

This work was supported by the German BMBF under Contract No. VDI/EKM 13N6917, by BRHE REC 007, by the Russian Science Support Foundation, and partly by the DFG via SFB 484 and the joint project with the RFBR under Contract No. 436RUS113/628.

[1] H. Yamada and Y. Ueda, J. Phys. Soc. Jpn. **68**, 2735 (1999).
[2] T. Yamauchi, Y. Ueda, and N. Mori, Phys. Rev. Lett. **89**, 057002 (2002);Y. Ueda, M. Isobe, and T. Yamauchi, J. Phys. Chem. Solids **63**, 951 (2002).
[3] H. Kobayashi, Bull. Chem. Soc. Jpn. **52**, 1315 (1979).
[4] A. D. Wadsley, Acta Crystallogr. **8**, 695 (1955).
[5] G. Obermeier *et al.*, Phys. Rev. B **66**, 085117 (2002).
[6] M. Itoh *et al.*, J. Phys. Chem. Solids **62**, 351 (2001).
[7] J.-I. Yamaura *et al.*, J. Phys. Chem. Solids **63**, 957 (2002).
[8] A. N. Vasil'ev *et al.*, Phys. Rev. B **64**, 174403 (2001).
[9] Y. Ueda *et al.*, J. Alloys Compd. **317-318**, 109 (2001).
[10] C. Presura *et al.*, Phys. Rev. Lett. **90**, 26402 (2003).
[11] K. Okazaki *et al.*, Phys. Rev. B **69**, 140506 (2004).
[12] S. Nishimoto and Y. Ohta, J. Phys. Soc. Jpn. **70**, 309 (2001).
[13] A. Friedrich *et al.*, J. Phys. (Paris) Lett. **39**, L343 (1978).
[14] T. Takahashi and H. Nagasawa, Solid State Commun. **39**, 1125 (1981).
[15] H. Nagasawa *et al.*, Mol. Cryst. Liq. Cryst. **86**, 195 (1982);M. Onoda, T. Takahashi, and H. Nagasawa, J. Phys. Soc. Jpn. **51**, 3868 (1982).
[16] M. Onoda and H. Nagasawa, J. Phys. Soc. Jpn. **52**, 2231 (1983).
[17] H.-A. Krug von Nidda *et al.*, Phys. Rev. B **65**, 134445 (2002).
[18] A. Abragam and B. Bleaney, *Electron Paramagnetic Resonance of Transition Ions* (Clarendon Press, Oxford, 1970).
[19] R. Kubo and K. Tomita, J. Phys. Soc. Jpn. **9**, 888 (1954).
[20] B. Pilawa, J. Phys. Condens. Matter **9**, 3779 (1997).
[21] R. M. Eremina *et al.*, Phys. Rev. B **68**, 014417 (2003).
[22] A. Bencini and D. Gatteschi, *Electron Paramagnetic Resonance of Exchange Coupled Systems* (Springer-Verlag, Berlin, 1990).
[23] M. Oshikawa and I. Affleck, Phys. Rev. B **65**, 134410 (2002).
[24] G. Grüner, *Density Waves in Solids* (Addison-Wesley, Reading, MA, 1994).